

The Hydroxide Complex of *Pseudomonas aeruginosa* Heme Oxygenase as a Model of the Low-Spin Iron(III) Hydroperoxide Intermediate in Heme Catabolism: ^{13}C NMR Spectroscopic Studies Suggest the Active Participation of the Heme in Macrocycle Hydroxylation

Gregori A. Caignan,[†] Rahul Deshmukh,[‡] Yuhong Zeng,[†] Angela Wilks,[‡]
Richard A. Bunce,[§] and Mario Rivera^{*†}

Contribution from the Department of Chemistry, The University of Kansas, Lawrence, Kansas 66045-7582, Department of Pharmaceutical Sciences, School of Pharmacy, University of Maryland, Baltimore, Maryland 21201-1180, and Department of Chemistry, Oklahoma State University, Stillwater, Oklahoma 74078

Received May 14, 2003; E-mail: mrivera@ku.edu

Abstract: ^{13}C NMR spectroscopic studies have been conducted with the hydroxide complex of *Pseudomonas aeruginosa* heme oxygenase ($\text{Fe}^{\text{III}}\text{-OH}$), where OH^- has been used as a model of the OOH^- ligand to gain insights regarding the elusive ferric hydroperoxide ($\text{Fe}^{\text{III}}\text{-OOH}$) intermediate in heme catabolism at ambient temperatures. Analysis of the heme core carbon resonances revealed that the coordination of hydroxide in the distal site of the enzyme results in the formation of at least three populations of $\text{Fe}^{\text{III}}\text{-OH}$ complexes with distinct electronic configurations and nonplanar ring distortions that are in slow exchange relative to the NMR time scale. The most abundant population exhibits a spin crossover between $S = 1/2$ and $S = 3/2$ spin states, and the two less abundant populations exhibit pure, $S = 3/2$ and $S = 1/2$, (d_{xy})¹ electronic configurations. We propose that the highly organized network of water molecules in the distal pocket of heme oxygenase, by virtue of donating a hydrogen bond to the coordinated hydroxide ligand, lowers its ligand field strength, thereby increasing the field strength of the porphyrin (equatorial) ligand, which results in nonplanar deformations of the macrocycle. This tendency to deform from planarity, which is imparted by the ligand field strength of the coordinated OH^- , is likely reinforced by the flexibility of the distal pocket in HO. These findings suggest that if the ligand field strength of the coordinated OOH^- in heme oxygenase is modulated in a similar manner, the resultant large spin density at the meso carbons and nonplanar deformations of the porphyrin ring prime the macrocycle to actively participate in its own hydroxylation.

Introduction

The enzyme heme oxygenase (HO) is intimately involved in the catabolism of heme. In this process, HO catalyzes the electron- and dioxygen-dependent breakdown of heme to biliverdin, iron, and carbon monoxide.¹ The catalytic cycle of HO (Scheme 1) starts when the ferric enzyme is reduced by NADPH cytochrome P450 reductase to its ferrous form, followed by the coordination of O_2 , which leads to the formation of an oxyferrous complex ($\text{Fe}^{\text{II}}\text{-O}_2$). The latter accepts a second electron from the reductase and is thereby transformed into the ferric hydroperoxy ($\text{Fe}^{\text{III}}\text{-OOH}$) oxidizing species,² which adds a hydroxyl group to the α -meso carbon to form α -meso-hydroxyheme (Scheme 1).^{3,4} Investigations of the reactivity of

HO toward peroxides and alkyl peroxides led to the conclusion that heme hydroxylation does not proceed via the formation of a high-valence compound I-like species.³ Rather, the terminal oxygen of the coordinated peroxide adds to a porphyrin meso carbon, which results in the formation of α -hydroxyheme. In fact, spectroscopic evidence supporting this conclusion was recently obtained by cryoreduction of the oxyferrous complex of HO to produce an intermediate, identified by EPR spectroscopy to be the $\text{Fe}^{\text{III}}\text{-OOH}$ complex, which upon warming is converted into the α -hydroxyheme complex.^{5,6} The α -meso-hydroxyheme complex of HO undergoes a subsequent O_2 -dependent elimination of the hydroxylated α -meso carbon as CO, with the simultaneous formation of verdoheme (Scheme

[†] The University of Kansas.

[‡] University of Maryland.

[§] Oklahoma State University.

(1) Tenhunen, R.; Marver, H. S.; Schmid, R. *J. Biol. Chem.* **1969**, *244*, 6388–6394.

(2) Yoshida, T.; Noguchi, M.; Kikuchi, G. *J. Biol. Chem.* **1980**, *255*, 4418–4420.

(3) Wilks, A.; Torpey, J.; Ortiz de Montellano, P. R. *J. Biol. Chem.* **1994**, *269*, 29553–29556.

(4) Ortiz de Montellano, P. R.; Wilks, A. *Adv. Inorg. Chem.* **2000**, *51*, 359–407.

(5) Davydov, R.; Macdonald, I. D. G.; Makris, T. M.; Sligar, S. G.; Hoffman, B. M. *J. Am. Chem. Soc.* **1999**, *121*, 10654–10655.

(6) Davydov, R.; Kofman, V.; Fujii, H.; Yoshida, T.; Ikeda-Saito, M.; Hoffman, B. M. *J. Am. Chem. Soc.* **2002**, *124*, 1798–1808.

with this approach is the very high reactivity of this key intermediate at ambient temperatures. To circumvent this problem, and as an initial attempt to study the chemical nature of the elusive $\text{Fe}^{\text{III}}\text{---OOH}$ intermediate in HO, we have undertaken a study in which hydroxide was used as a model of the hydroperoxide ligand. As will be shown below, we find that the hydroxide complex of HO ($\text{Fe}^{\text{III}}\text{---OH}$) has properties that are distinct from the planar ($d_{7\pi}$) hydroxide complexes characteristic of globins and peroxidases in that the heme in $\text{Fe}^{\text{III}}\text{---OH}$ acquires unusual electronic structures that strongly suggest nonplanar distortions.

Experimental Section

Protein Preparation and Reconstitution with ^{13}C -Labeled Heme. Heme oxygenase from *Pseudomonas aeruginosa* (*pa*-HO) was expressed and purified as described previously.^{17,18} ^{13}C -labeled δ -amino-levulinic acids (ALA) were used as biosynthetic precursors for the preparation of protoheme IX (heme) according to previously described methodology.^{19,20} $[5\text{-}^{13}\text{C}]\text{-}\delta$ -Aminolevulinic acid ($[5\text{-}^{13}\text{C}]\text{-ALA}$) and $[4\text{-}^{13}\text{C}]\text{-ALA}$ were synthesized according to methodology described previously.²¹ $[5\text{-}^{13}\text{C}]\text{-ALA}$ was used to prepare heme labeled at the meso (C_m) and α -pyrrole (C_α) carbons shown in Figure 5A, and $[4\text{-}^{13}\text{C}]\text{-ALA}$ was utilized to prepare heme labeled at the C_α and β -pyrrole (C_β) carbons shown in Figure 5B. Isotopically labeled heme is initially purified in its complex with rat liver outer membrane (OM) cytochrome b_5 .^{19,20} ^{13}C -labeled heme is extracted from OM cytochrome b_5 as follows: While the temperature is maintained at 4 °C, 15 mL of pyridine is added to 2.5 mL of rat OM cytochrome b_5 (1 mM) dissolved in phosphate buffer ($\mu = 0.1$, pH = 7.0). Slow addition of chloroform (10–15 mL) typically results in the precipitation of the polypeptide, while maintaining the pyridine hemochrome in the supernatant. The latter is separated from the precipitate by centrifugation, allowed to equilibrate at room temperature, and then dried over anhydrous MgSO_4 . The desiccant is separated by filtration, and the solution is evaporated to dryness with the aid of a rotary evaporator. The solid is redissolved in 3–4 mL of dimethyl sulfoxide, and the resultant solution is immediately used to reconstitute HO. To this end, a solution (20 mL) containing approximately 2 μmol of *pa*-HO is titrated with the solution containing ^{13}C -labeled heme until the ratio A_{280}/A_{Soret} no longer changes. The resultant solution is incubated at 4 °C overnight and subsequently purified in a Sephadex G-50 column (3 cm \times 100 cm), previously equilibrated with phosphate buffer, $\mu = 0.10$ and pH = 7.0.

Spectroscopic Studies. ^1H and ^{13}C NMR spectra were acquired on a Varian Unity Inova spectrometer operating at frequencies of 598.611 and 150.532 MHz, respectively. ^1H spectra were referenced to the residual water peak at 4.8 ppm, and ^{13}C spectra were referenced to an external solution of dioxane (60% v/v in D_2O) at 66.66 ppm. ^1H spectra from high-spin HO were acquired with presaturation of the residual water peak over 137 kHz, with a 125 ms acquisition time, a 25 ms relaxation delay, and 2048 scans. Spectra from low-spin HO were also acquired with presaturation of the residual water peak, with an acquisition time of 250 ms, and a 25 ms relaxation delay, over a spectral width of 30 kHz. ^{13}C NMR spectra were typically collected from solutions containing approximately 5 mM HO in 50 mM borate buffer at pH 10.3; the pH readings have not been corrected for the deuterium isotope effect. The samples were concentrated to 250 μL in centrifugal

concentrators equipped with 10 000 molecular weight cutoff membranes (Centricon-Millipore Co, Bedford, MA) and then transferred to Shigemi NMR tubes (5 mm) with susceptibilities matched to D_2O (Shigemi, Inc., Allison Park, PA). ^{13}C spectra were acquired over 48 K data points, with a spectral width of 300 kHz, an acquisition time of 80 ms, and no relaxation delay; typically, 1 000 000 scans were obtained in approximately 24 h.

The conversion of high-spin aquo ($\text{Fe}^{\text{III}}\text{---H}_2\text{O}$) to low-spin hydroxo ($\text{Fe}^{\text{III}}\text{---OH}$) *pa*-HO was also monitored by electronic absorption spectroscopy, with the aid of a UV-vis S2000 spectrophotometer (Ocean Optics, Dunedin, FL). To this end, a solution of $\text{Fe}^{\text{III}}\text{---H}_2\text{O}$ in water (pH 6.3) was placed in a quartz cuvette (1-cm path length) where it was stirred continuously with the aid of a magnetic bar. This solution was titrated with 0.2 M sodium hydroxide, monitoring the pH and the electronic absorption spectrum after the addition of each aliquot of base. The data from this titration were fitted to the Henderson-Hasselbalch equation to obtain the $\text{p}K_a$ for the deprotonation of the coordinated water.

Circular dichroism spectra were measured with the aid of a JASCO J-810 spectropolarimeter in the far UV-region (190–250 nm, 0.2 mm resolution, 1.0 mm bandwidth) at 25 °C in 10 mM potassium phosphate buffers at pH 6.0, 8.0, or 10.0 with a protein concentration of 5 μM . The molar ellipticity ($\text{deg cm}^2 \text{dmol}^{-1}$) in the far UV region was calculated directly using the JASCO standard software analysis following subtraction of the baseline spectra.

Results and Discussion

Characterization of the Hydroxide Complex of *pa*-HO by ^1H NMR and Electronic Absorption Spectroscopy. The electronic absorption spectra in Figure 1A were obtained upon titration of a solution of *pa*-HO from pH 6.3 to pH 10.3. The Soret band shifts from 406 nm at pH 6.3 to 415 nm at pH 10.3, concomitant with the emergence of α and β bands at 540 and 574 nm, respectively. The band at 630 nm, which is typically considered a high-spin marker, is clearly present at pH 6.3 but gradually disappears as the pH is increased, until it is no longer detectable at pH 10.3. These pH-dependent changes in the electronic absorption spectra of *pa*-HO exhibit well-defined isosbestic points at 482, 524, and 610 nm that are indicative of the equilibrium between the high-spin $\text{Fe}^{\text{III}}\text{---H}_2\text{O}$ and the low-spin $\text{Fe}^{\text{III}}\text{---OH}$ complexes shown in Figure 1; the $\text{p}K_a$ for the deprotonation of the coordinated water is 8.3. The CD spectra obtained at pH 6.0 and 10.0 (Figure 1B) are essentially superimposable and therefore demonstrate that the fold of *pa*-HO is not affected upon increasing the pH of the solution. On the basis of the above-described observations, it is possible to conclude that a stable $\text{Fe}^{\text{III}}\text{---OH}$ complex is formed at pH values above 9.3.

The formation and properties of the hydroxide complex of *pa*-HO have also been studied by ^1H NMR spectroscopy. Thus, the ^1H NMR spectrum obtained at pH 6.3 (Figure 2a) displays heme-methyl resonances between 60 and 80 ppm, which are typical of high-spin heme active sites, where the ferric ion is axially coordinated by a His and H_2O ligands²² ($\text{Fe}^{\text{III}}\text{---H}_2\text{O}$). As the pH of the solution is increased, the relative intensity of these peaks decreases with the concomitant emergence and growth of heme-methyl peaks near 20 ppm that originate from the low-spin $\text{Fe}^{\text{III}}\text{---OH}$ complex. The fact that at pH values intermediate between 6 and 10 (Figure 2b and c) one can observe peaks originating from heme-methyl groups in the high-

- (17) Ratliff, M.; Zhu, W.; Deshmukh, R.; Wilks, A.; Stojilkovic, I. *J. Bacteriol.* **2001**, *183*, 6394–6403.
 (18) Caignan, G. A.; Deshmukh, R.; Wilks, A.; Zeng, Y.; Huang, H.; Moenne-Loccoz, P.; Bunce, R. A.; Eastman, M. A.; Rivera, M. *J. Am. Chem. Soc.* **2002**, *124*, 14879–14892.
 (19) Rivera, M.; Walker, F. A. *Anal. Biochem.* **1995**, *230*, 295–302.
 (20) Rivera, M.; Qiu, F.; Bunce, R. A.; Stark, R. E. *J. Biol. Inorg. Chem.* **1999**, *4*, 87–98.
 (21) Bunce, R. A.; Shilling, C. L., III; Rivera, M. *J. Labelled Compd. Radiopharm.* **1997**, *39*, 669–675.

- (22) La Mar, G. N.; Satterlee, J. D.; De Ropp, J. S., Eds.; *Nuclear Magnetic Resonance of Hemoproteins*; Academic Press: New York, 2000; Vol. 5.

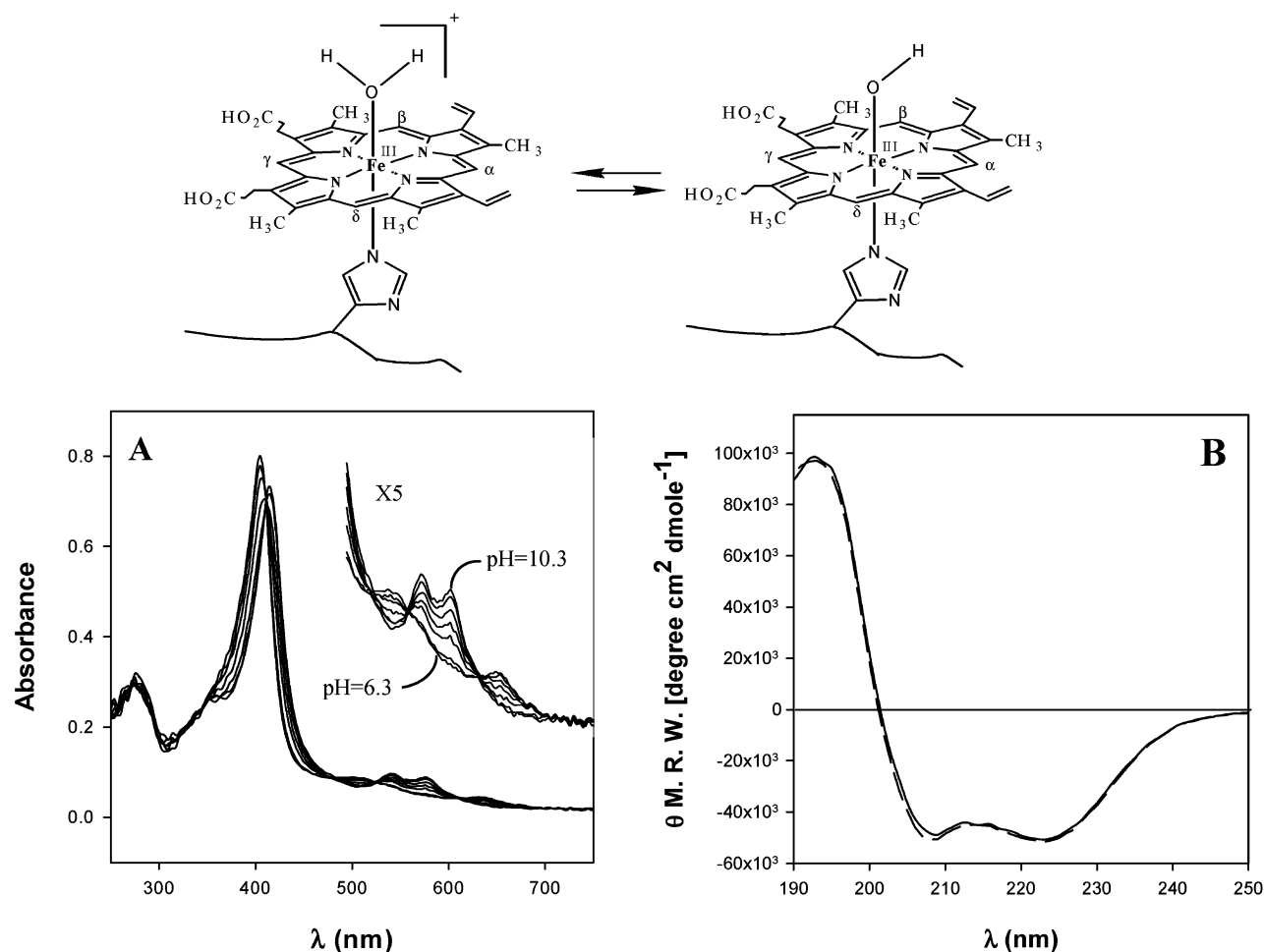


Figure 1. (A) Electronic absorption spectra obtained during the titration of ferric HO with sodium hydroxide. (B) CD spectra obtained at pH 6.5 (dashed line) and pH 10.0 (solid). The spectrum obtained at pH 8.5 is identical to those shown in the figure but has not been included for clarity.

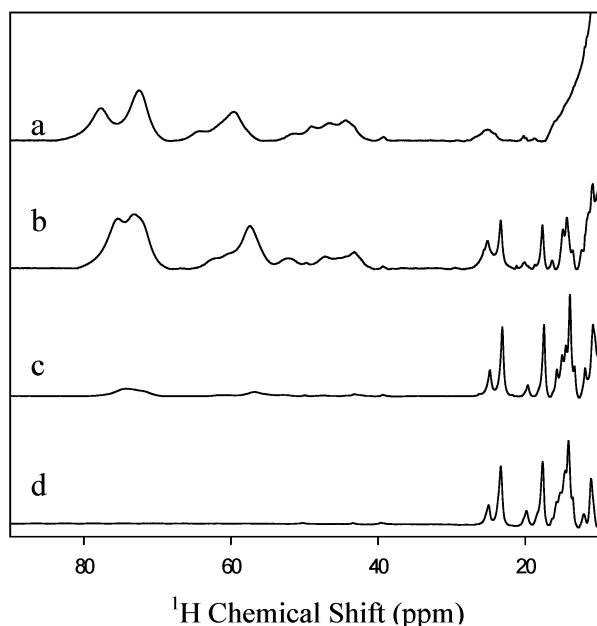


Figure 2. Downfield portion of the ^1H NMR spectra of *pa*-HO obtained at 25 °C and pH 6.3 (a), 8.3 (b), 9.3 (c), and 10.3 (d).

spin $\text{Fe}^{\text{III}}-\text{H}_2\text{O}$, as well as those from the low-spin $\text{Fe}^{\text{III}}-\text{OH}$ complexes in the same spectrum, indicates that these two species are in slow exchange relative to the NMR time scale. Consider-

ing the maximum and minimum differences between the high-spin and low-spin heme-methyl ^1H signals, we could estimate the NMR time scale to be $\sim 7 \times 10^4 \text{ s}^{-1}$. On the other hand, the ^1H NMR spectrum obtained at pH 10.3 (Figure 2d) does not exhibit heme-methyl peaks in the region between 60 and 80 ppm, thus demonstrating the quantitative conversion of the high-spin $\text{Fe}^{\text{III}}-\text{H}_2\text{O}$ species to the low-spin $\text{Fe}^{\text{III}}-\text{OH}$ complex.

The high- and low-frequency portions of the ^1H NMR spectrum of the $\text{Fe}^{\text{III}}-\text{OH}$ complex of *pa*-HO (pH 10.3) are shown in Figure 3a. This spectrum is different from that obtained from the cyanide complex of *pa*-HO ($\text{Fe}^{\text{III}}-\text{CN}$) at pH 7.4 (Figure 3b) in that the heme-methyl peaks are shifted to lower frequencies (upfield) and the vinyl- β resonances, which in the $\text{Fe}^{\text{III}}-\text{CN}$ complex are near -8 ppm, are shifted to higher frequencies (downfield) and therefore are no longer discernible from the large envelope of protein resonances. The ^1H NMR spectrum of the $\text{Fe}^{\text{III}}-\text{CN}$ complex at pH 7.4 revealed the presence of heme-methyl groups from major (Me) and minor (me) heme orientational isomers.¹⁸ The ^1H NMR spectrum of the $\text{Fe}^{\text{III}}-\text{OH}$ complex at pH 10.3 also suggests the presence of major and minor heme orientational isomers. The smaller shifts of the heme methyl and heme vinyl- β protons from the $\text{Fe}^{\text{III}}-\text{OH}$ complex can, in principle, be interpreted as an indication of a change in the conformation of the proximal His ligand. However, this hypothesis was discarded by studying the ^1H NMR spectrum of the $\text{Fe}^{\text{III}}-\text{CN}$ complex at pH 10.3 (see

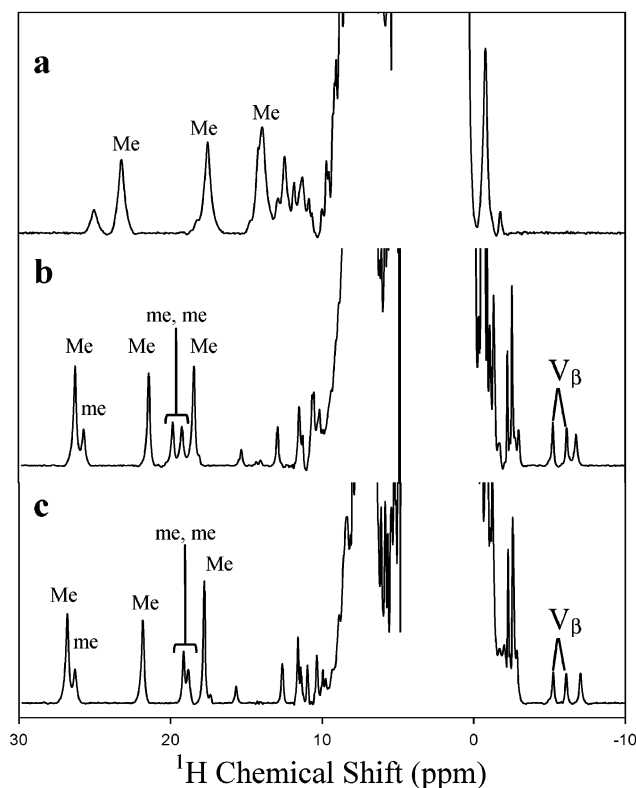


Figure 3. ^1H NMR spectra of (a) $\text{Fe}^{\text{III}}\text{-OH}$ at pH 10, (b) $\text{Fe}^{\text{III}}\text{-CN}$ at pH 7.4, and (c) $\text{Fe}^{\text{III}}\text{-CN}$ at pH 10.3 obtained at 25 °C. Me and me represent heme-methyl resonances from major and minor heme orientational isomers, respectively.

Figure 3c), which was obtained after 3 equiv of NaCN was added to a solution of the $\text{Fe}^{\text{III}}\text{-OH}$ complex at pH 10.3. This spectrum shows that the chemical shifts corresponding to heme methyl and heme vinyl- β protons of the $\text{Fe}^{\text{III}}\text{-CN}$ complex at pH 10.3 are almost identical to the corresponding resonances of the $\text{Fe}^{\text{III}}\text{-CN}$ complex at pH 7.4, therefore strongly suggesting that the conformation of the proximal His ligand and the seating of the heme have not been perturbed at pH 10.3. Furthermore, when these observations are taken together with those made from the electronic absorption and CD spectroscopic studies, it becomes evident that at pH 10.3 the $\text{Fe}^{\text{III}}\text{-OH}$ complex must exhibit a fold nearly identical to that of the $\text{Fe}^{\text{III}}\text{-H}_2\text{O}$ complex. The more compressed shifts of the heme methyl and heme vinyl- β protons in the spectrum of $\text{Fe}^{\text{III}}\text{-OH}$, therefore, are suggestive of an electronic structure different from the typical low-spin d_{xy} configuration. In fact, it will be shown below that the core carbon resonances of $\text{Fe}^{\text{III}}\text{-OH}$ indicate that this species does not exist in the common low-spin d_{xy} electronic structure typical of the hydroxide complex of globins.

^{13}C NMR Chemical Shifts Are Diagnostic of Heme Electronic Structure. ^{13}C NMR spectroscopy is emerging as a powerful experimental tool to study the electronic structure of model hemes. Studies conducted with low-spin ferriheme complexes established that chemical shifts originating from porphyrin core carbons, C_α , C_β , and C_m , permit the relatively straightforward assessment of electronic structure.^{23–27} The

schematic representations of Figure 4 summarize the relationships between ^{13}C chemical shifts and electronic configurations that are relevant to this study: (1) Spin delocalization in ferrihemes with the common $S = 1/2$, d_{xy} electronic structure, which are typically planar, is mainly into the porphyrin $3e(\pi)$ orbital shown schematically in Figure 4. It can be seen from the relative sizes of the circles in the schematic representation of the $3e(\pi)$ orbital that the C_β carbons possess relatively large electron density, the C_α carbons possess relatively small electron density, and the C_m carbons have zero electron density. As a consequence, low-spin d_{xy} ferrihemes exhibit C_β resonances at ~ 200 ppm, C_α resonances at ~ 100 ppm, and C_m signals near 50 ppm^{20,23} (Figure 4a). (2) Spin delocalization in ferrihemes with the less common $S = 1/2$, $(d_{xy})^1$ electronic configuration is mainly into the $3a_{2u}(\pi)$ orbital,²⁸ which exhibits large electron density at the C_m carbons and small electron density at the C_α and C_β carbons (Figure 4). Ferrihemes possessing the $(d_{xy})^1$ electron configuration (typically ruffled) exhibit large downfield C_m shifts (~ 1000 ppm), relatively large upfield C_α shifts (~ -300 ppm), and negligible C_β shifts ($\sim 20\text{--}70$ ppm)²⁴ (see Figure 4b). The large downfield C_m shifts are a consequence of delocalization of unpaired electron density from the d_{xy} orbital into the porphyrin $3a_{2u}(\pi)$ orbital of the ruffled porphyrin.¹³ Because the $3a_{2u}(\pi)$ orbital has negligible spin density at the C_α position, the relatively large upfield C_α shifts are a consequence of spin polarization from the C_m carbons.²⁴ Unpaired electron density from the d_{xy} orbital can be delocalized into the $3a_{2u}(\pi)$ orbital only if the macrocycle is significantly ruffled, so that the nodal planes of the p_z orbital are no longer in the xy plane and projections of these p_z orbitals have the proper symmetry to interact with the d_{xy} orbital¹³ (see Figure 4). (3) Ferrihemes possessing the $S = 3/2$, $(d_{xy})^2(d_{xz}, d_{yz})^2(d_z^2)^1$ spin state are also markedly nonplanar and exhibit complicated distortions from nominal D_{4h} symmetry,^{29,30} which suggests that these ferriheme complexes might exist in solution as a complex mixture of interconverting conformers with similar energies. Nonplanar hexacoordinated $\text{Fe}^{\text{III}}\text{-porphyrinates}$ possessing the $S = 3/2$ spin state exhibit a unique pattern of ^{13}C NMR shifts³¹ with very large downfield C_β shifts (~ 1000 ppm), large downfield C_α shifts (~ 600 ppm), and large upfield C_m shifts (~ -300 ppm) (Figure 4c). The large downfield shifts of the C_α and C_β carbons are consistent with the presence of unpaired electron density in each of the d_{xz} and d_{yz} orbitals, which are delocalized into the $3e(\pi)$ porphyrin orbital. Because this porphyrin orbital has zero electron density at the meso carbons, the large upfield C_m shift is a consequence of spin polarization from the neighboring C_α carbon.^{24,27}

The application of ^{13}C NMR spectroscopy to the study of heme electronic structure in proteins and enzymes is less common because the relatively low sensitivity and low natural abundance of ^{13}C make the observation of paramagnetically

(23) Mispelter, J.; Momenteau, M.; Lhoste, J. M. In *Biological Magnetic Resonance*; Reuben, J., Ed.; Plenum Press: New York, 1993; Vol. 12, pp 299–355.

(24) Ikeue, T.; Ohgo, Y.; Takashi, S.; Nakamura, M.; Fujii, H.; Yokoyama, M. *J. Am. Chem. Soc.* **2000**, *122*, 4068–4076.

(25) Ikeue, T.; Ohgo, Y.; Saitoh, T.; Yamaguchi, T.; Nakamura, M. *Inorg. Chem.* **2001**, *40*, 3423–3434.

(26) Ikezaki, A.; Nakamura, M. *Inorg. Chem.* **2002**, *41*, 6225–6236.

(27) Ikeue, T.; Ohgo, Y.; Yamaguchi, M.; Takahashi, M.; Takeda, M.; Nakamura, M. *Angew. Chem., Int. Ed.* **2001**, *40*, 2617–2620.

(28) Walker, F. A. In *The Porphyrin Handbook*; Guillard, R., Ed.; Academic Press: New York, 2000; Vol. 5, pp 81–183.

(29) Ikeue, T.; Saitoh, T.; Yamaguchi, T.; Ohgo, Y.; Nakamura, M.; Takahashi, M.; Takeda, M. *Chem. Commun.* **2000**, 1989–1990.

(30) Simonato, J. P.; Pécaut, J.; Le Pape, L.; Oddou, J. L.; Jeandey, C.; Shang, M.; Scheidt, R.; Wojcieszynski, J.; Wolowicz, S.; Latos-Grazyznsky, L.; Marchon, J. C. *Inorg. Chem.* **2000**, *39*, 3978–3987.

(31) Ikeue, T.; Ohgo, Y.; Yamaguchi, M.; Takahashi, M.; Takeda, M.; Nakamura, M. *Angew. Chem., Int. Ed.* **2001**, *40*, 2617–2620.

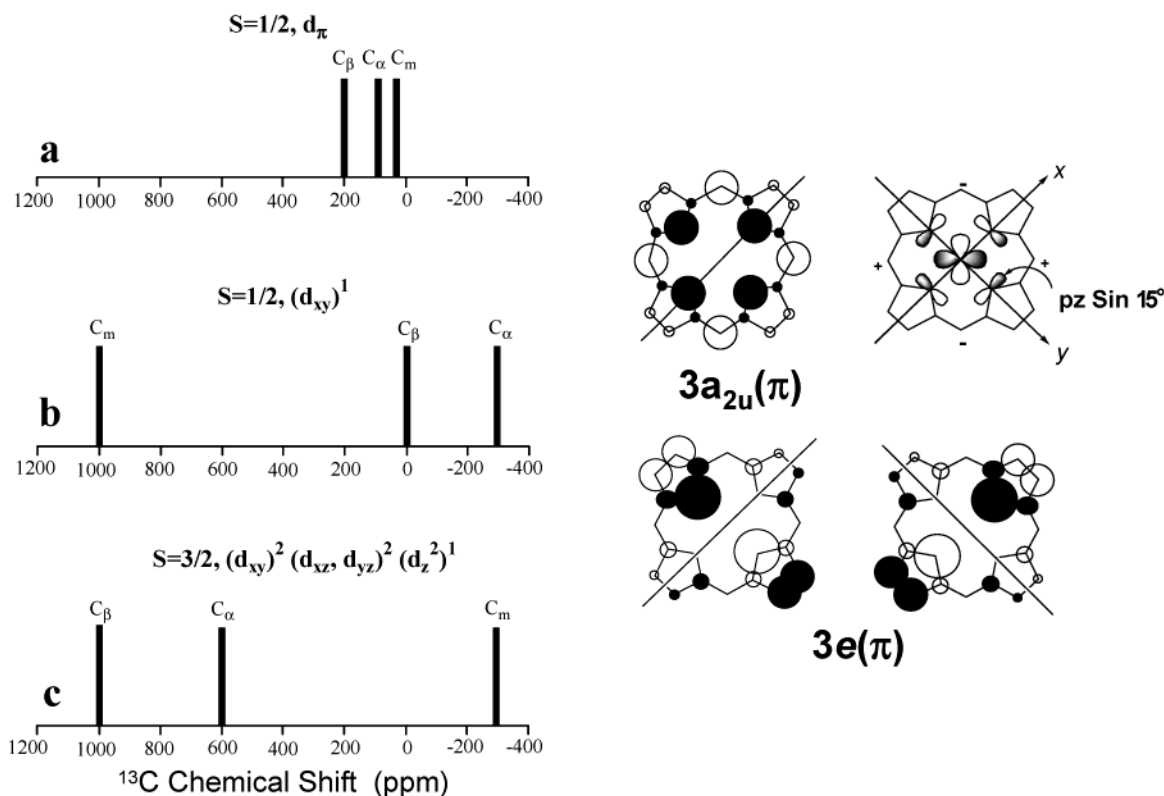


Figure 4. Left: Typical porphyrin core carbon chemical shifts for (a) Fe^{III}–porphyrinates with the $S = 1/2$, d_{π} electron configuration, (b) Fe^{III}–porphyrinates with the $S = 1/2$, $(d_{xy})^1$ electron configuration, and (c) Fe^{III}–porphyrinates with the $S = 3/2$, $(d_{xy})^2 (d_{xz}, d_{yz})^2 (d_z)^2)^1$ electron configuration. Right: Schematic representation (adapted from ref 15) of the $3a_{2u}(\pi)$ and $3e(\pi)$ porphyrin orbitals. The relative sizes of the circles at each atom are proportional to the calculated electron density. The possible interactions between the d_{xy} orbital and the porphyrin nitrogens of a ruffled porphyrin which allow spin delocalization into the $3a_{2u}(\pi)$ orbital are shown schematically next to this orbital.

affected ¹³C resonances more demanding. This limitation is felt more strongly when one is interested in observing porphyrin C_α and C_β carbons because it is not possible to take advantage of directly attached protons to capitalize on the increased sensitivity of the inverse-detection experiments.³² To overcome these problems, we have developed a biosynthetic method that allows the efficient preparation of ¹³C-labeled heme from judiciously labeled ALA,²¹ the first committed precursor in heme biosynthesis, by adequate manipulation of an expression system that overproduces the heme binding protein OM cytochrome *b*₅.^{19,33} Heme in OM cytochrome *b*₅ is not covalently attached to the polypeptide. Therefore, ¹³C-labeled heme can be extracted and used to reconstitute other proteins of interest. This strategy has been successfully applied to study a complex mixture of heme orientational and heme rotational isomers present in a solution of *pa*-HO mutants.¹⁸ In the study reported herein, we have used heme labeled with ¹³C at the core carbons to study the electronic structure of the Fe^{III}–OH complex. Observation of the corresponding core carbon resonances revealed the presence of a mixture of Fe^{III}–OH populations which differ in their electronic structure and degree of nonplanar porphyrin distortions. It is noteworthy that this information, which is directly attainable from the ¹³C NMR shifts, is not easily obtained by other spectroscopic means.

¹³C NMR Spectroscopy Reveals the Coexistence of at Least Three Spin States Exhibiting Different Degrees of

Population of the Iron- d_{π} Orbitals. A portion of the ¹³C NMR spectrum of Fe^{III}–OH reconstituted with heme labeled at the C_m and C_α carbons is depicted in Figure 5A. If the pH of the solution is decreased from 10.3 to 6.3, the sets of highlighted resonances near 50 and 450 ppm become less intense until at pH values below 7.0 they become unobservable (see Supporting Information Figure S1). Subsequent increase of the solution pH results in the appearance and growth of the set of resonances near 50 and 450 ppm, and at pH 10.3 the spectrum shown in Figure 5A is restored. This behavior is consistent with the reversible equilibrium between the Fe^{III}–H₂O and Fe^{III}–OH complexes of *pa*-HO shown in Figure 1.

The electronic absorption and ¹H NMR spectra of the Fe^{III}–OH complex suggest a low-spin electronic configuration for this species. However, the fact that resonances from core porphyrin carbons in Figure 5A appear near 450 ppm strongly suggests that the electronic configuration of the Fe^{III}–OH complex is not the common low-spin d_{π} . Indeed, model hemes and hemoproteins possessing a low-spin d_{π} electronic configuration give rise to ¹³C NMR spectra displaying C_m resonances between 5 and 50 ppm, C_α resonances between –10 and 100 ppm, and C_β resonances between 150 and 250 ppm^{18,20,23,34} (see Figure 4b). On the other hand, if the set of resonances at ca. 450 ppm can be attributed to meso carbons, it would then be possible to conclude that the electronic structure of the Fe^{III}–OH complex of *pa*-HO is $S = 1/2$, $(d_{xy})^1$. However, it is important to note that when [5-¹³C]-ALA is used as a precursor of heme

(32) Summers, M. F.; Marzilli, L. G.; Bax, A. *J. Am. Chem. Soc.* **1986**, *108*, 4285–4294.

(33) Qiu, F.; Rivera, M.; Stark, R. E. *J. Magn. Reson.* **1998**, *130*, 76–81.

(34) Goff, H. M. *J. Am. Chem. Soc.* **1981**, *103*, 3714–3722.

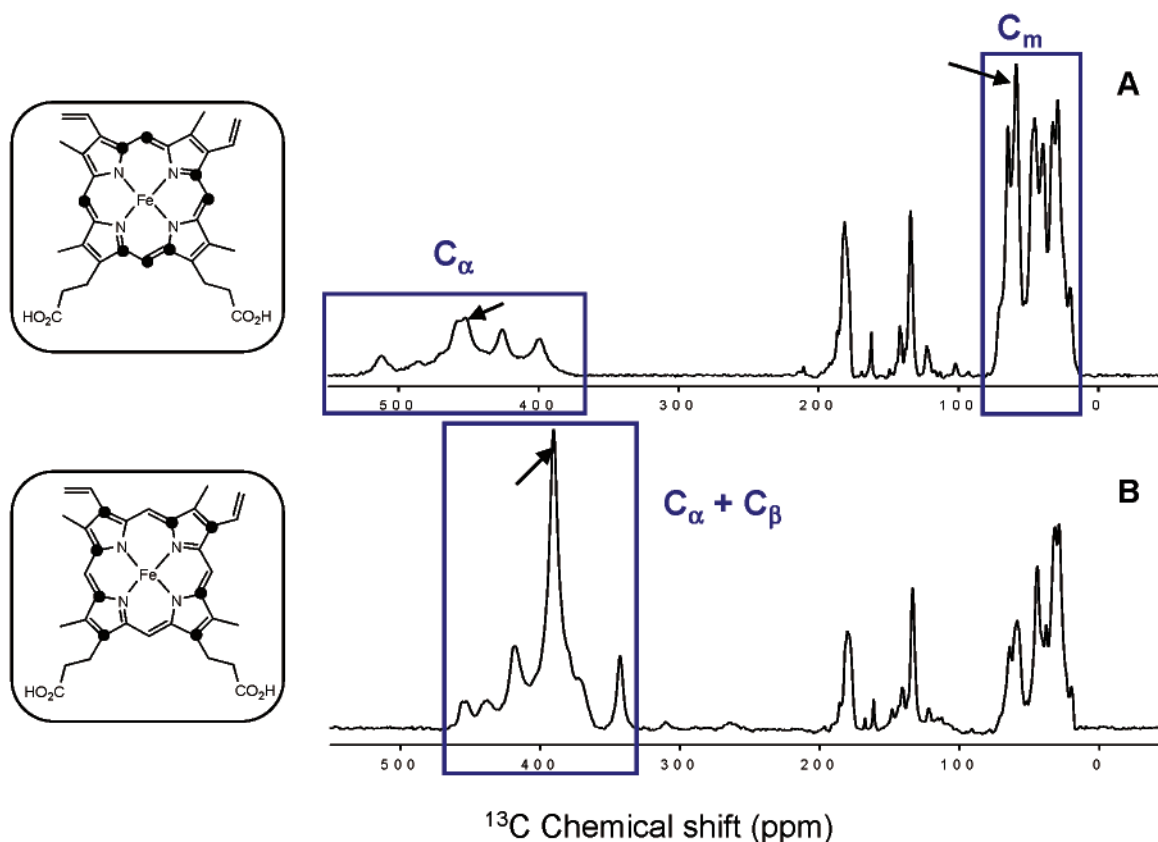


Figure 5. A portion of the ^{13}C NMR spectra obtained at 37 °C from a solution of the $\text{Fe}^{\text{III}}\text{-OH}$ complex of *pa*-HO (pH 10.3) reconstituted with heme labeled at the C_α and C_m carbons (A) and C_α and C_β carbons (B). The labeled carbons are highlighted by (●) in the structures shown to the left of each corresponding spectrum. The chemical shifts of the peaks highlighted by an arrow have been used to construct the temperature dependence plot of Figure 6.

biosynthesis the C_m and C_α carbons shown in Figure 5A are labeled.²⁰ Consequently, to determine the electronic configuration of the $\text{Fe}^{\text{III}}\text{-OH}$ complex, it is necessary to elucidate whether the set of resonances at 450 ppm in Figure 5A originate from C_m or from C_α carbons. To this end, $[4\text{-}^{13}\text{C}]\text{-ALA}$ was used to label the C_α and C_β carbons shown in Figure 5B, and the labeled heme was used to reconstitute the $\text{Fe}^{\text{III}}\text{-OH}$ complex of *pa*-HO. The corresponding ^{13}C NMR spectrum displays a set of resonances between 350 and 450 ppm, whereas the region near 50 ppm only shows peaks originating from the polypeptide. These observations suggest that both the C_α and the C_β carbons of the $\text{Fe}^{\text{III}}\text{-OH}$ complex resonate between 350 and 500 ppm, therefore implying that the set of resonances near 450 ppm in Figure 5A originate from C_α carbons and that the set of accompanying resonances near 50 ppm arise from C_m carbons.

It is evident that the chemical shifts from the C_α , C_β , and C_m carbons shown in Figure 5 are not consistent with a low-spin (d_{xy})¹ electronic configuration because ferrihemes with this electronic structure place significant unpaired electron density at the C_m carbons. This results in large downfield (~ 1000 ppm) C_m shifts and, by spin polarization, relatively large upfield (~ -300 ppm) C_α shifts (see Figure 4b). On the other hand, the C_α and C_β chemical shifts depicted in Figure 5 are reminiscent of the recently reported $S = 1/2$, $S = 3/2$ spin state crossover that is characterized by C_α and C_β carbon shifts between 300 and 600 ppm and C_m chemical shifts near 0 ppm.^{27,35} The C_α and C_β resonances shown in Figure 5 exhibit

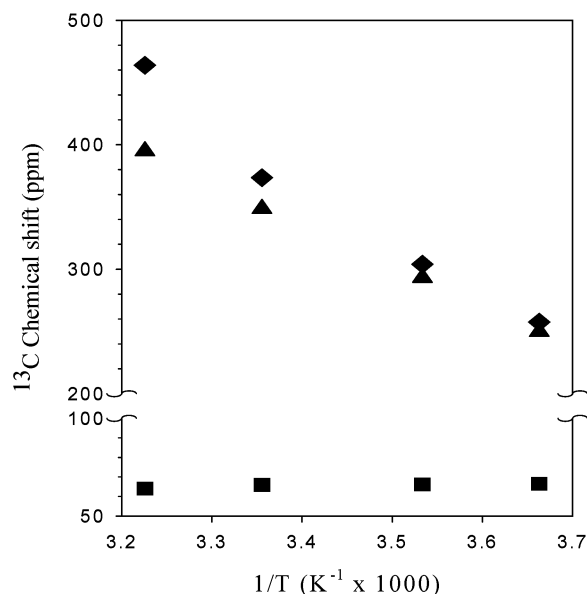


Figure 6. Temperature dependence of the C_α (◆), C_β (▲), and C_m (■) chemical shifts for the $\text{Fe}^{\text{III}}\text{-OH}$ complex of *pa*-HO. The plot was constructed with chemical shifts corresponding to those peaks highlighted with an arrow in Figure 5A and B.

a pronounced temperature dependence that shifts the C_α carbons from ~ 260 ppm at 0 °C to ~ 460 ppm at 37 °C, and the C_β carbons from ~ 250 ppm at 0 °C to ~ 400 ppm at 37 °C (Figure 6). It is therefore possible to rationalize the shifts in Figure 5 assuming that at 37 °C there is approximately $1/3 S = 3/2$,

(35) Ohgo, Y.; Ikewe, T.; Nakamura, M. *Inorg. Chem.* **2002**, *41*, 1698–1700.

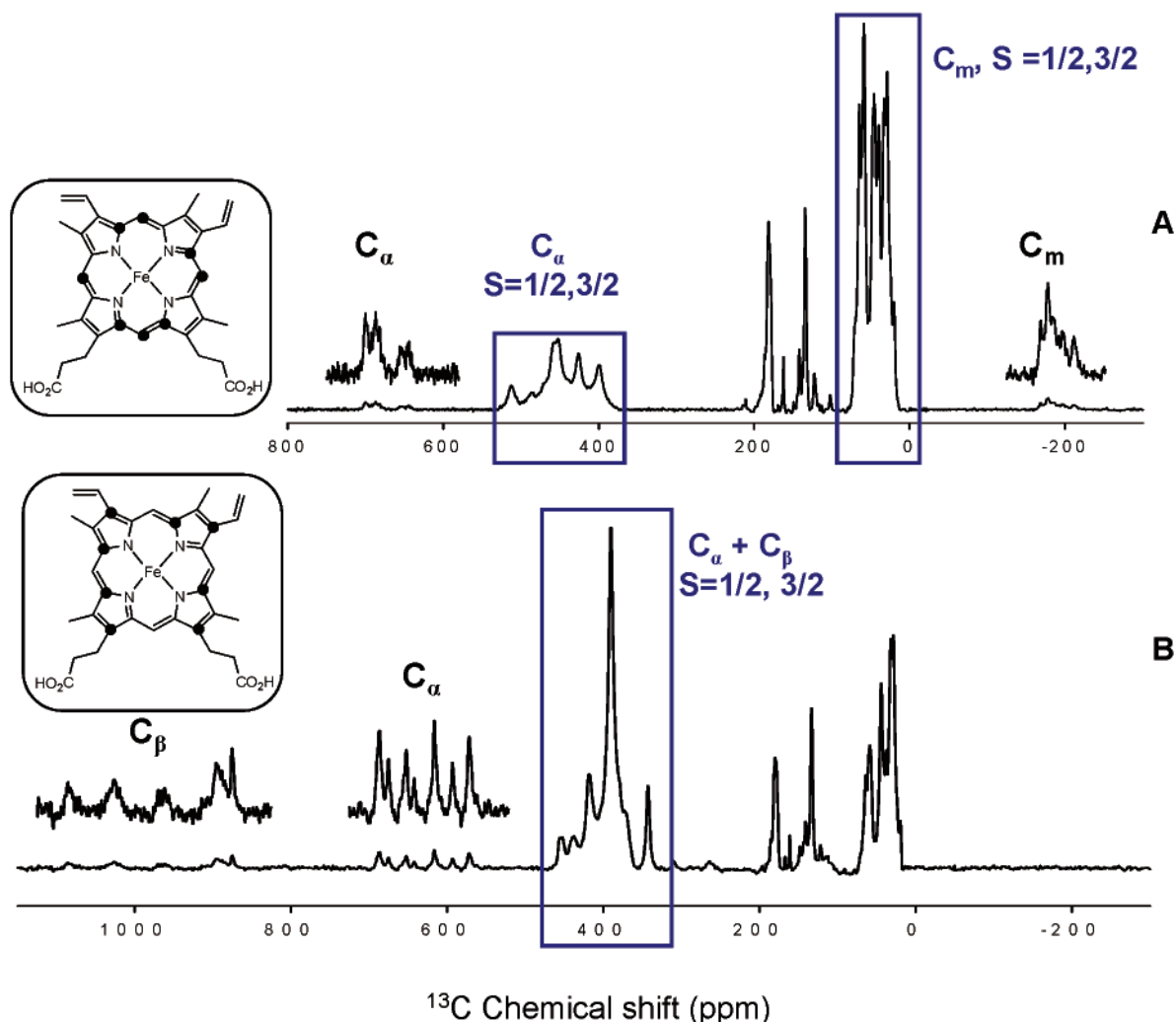


Figure 7. A portion of the ^{13}C NMR spectra obtained at 37 °C from a solution of the $\text{Fe}^{\text{III}}\text{-OH}$ complex of *pa*-HO (pH 10.3) reconstituted with heme labeled at the C_α and C_m (A) and C_α and C_β carbons (B). Peaks corresponding to the population with the $S = 1/2$, $S = 3/2$ spin state crossover are highlighted in a blue box (see Figure 5).

$(d_{xy})^2(d_{xz}, d_{yz})^2(d_z)^1$ and approximately $2/3 S = 1/2$, d_π contribution. As the temperature is lowered, the contribution of $S = 1/2$, d_π increases, and the core carbon chemical shifts approach the values expected for an $S = 1/2$, d_π Fe^{III} -porphyrinate. This behavior of the core carbon chemical shifts in response to changes in temperature is in agreement with that of Fe^{III} -porphyrinates known to exhibit the $S = 1/2$, $S = 3/2$ spin state crossover.³¹ It is not yet clear why the chemical shifts of the C_m carbons exhibit a shallow temperature dependence. The alternative equilibrium between the $S = 1/2$, $(d_{xy})^1$ and $S = 3/2$, $(d_{xz}, d_{yz})^3(d_{xy})^1(d_z)^1$ can be ruled out on the basis of the temperature-dependent changes of the core carbon chemical shifts because at the lower temperatures one would expect the main contribution to be from the $S = 1/2$, $(d_{xy})^1$ ground state. Thus, at the lower temperatures, the C_m shifts should be large and positive (downfield), and the C_α shifts should be negative, with the C_β shifts near 50 ppm.

Figure 7A depicts a larger spectral window of the ^{13}C NMR spectrum obtained from the $\text{Fe}^{\text{III}}\text{-OH}$ complex reconstituted with heme labeled at the C_α and C_m carbons. It is apparent that, in addition to the peaks described above (blue box), there are additional resonances near 650 and -200 ppm. Although these resonances clearly originate from C_α and C_m carbons, it is not

possible to assign them to their corresponding core carbons solely on the basis of this spectrum. To circumvent this problem, it is again useful to consider the spectrum obtained from the $\text{Fe}^{\text{III}}\text{-OH}$ complex reconstituted with heme labeled at the C_α and C_β carbons (Figure 7B). Inspection of this spectrum clearly shows that the region near -200 ppm is devoid of peaks, thus implying that the resonances near -200 ppm in the spectrum obtained from enzyme reconstituted with heme labeled at the C_α and C_m carbons (Figure 7A) can be assigned to meso carbons. In the same vein, the peaks near 650 ppm in the spectra of Figure 7A and B must originate from C_α carbons, and the peaks centered near 1000 ppm in the spectrum of Figure 7B must originate from C_β carbons. The large downfield shifts for α - and β -pyrrole carbons, accompanied by upfield shifted meso carbons, are characteristic of an $S = 3/2$ spin state,²⁷ where unpaired electron density in the d_{xz} and d_{yz} orbitals is delocalized into the α - and β -pyrrole carbons via the $3e(\pi)$ porphyrin orbital (see Figure 4). This orbital exhibits zero electron density at the meso carbons; thus the large upfield C_m shifts have been ascribed to spin polarization from the neighboring C_α carbon atoms.^{24,27}

Figure 8A depicts the entire ^{13}C NMR spectrum of the $\text{Fe}^{\text{III}}\text{-OH}$ complex of *pa*-HO reconstituted with heme labeled at the

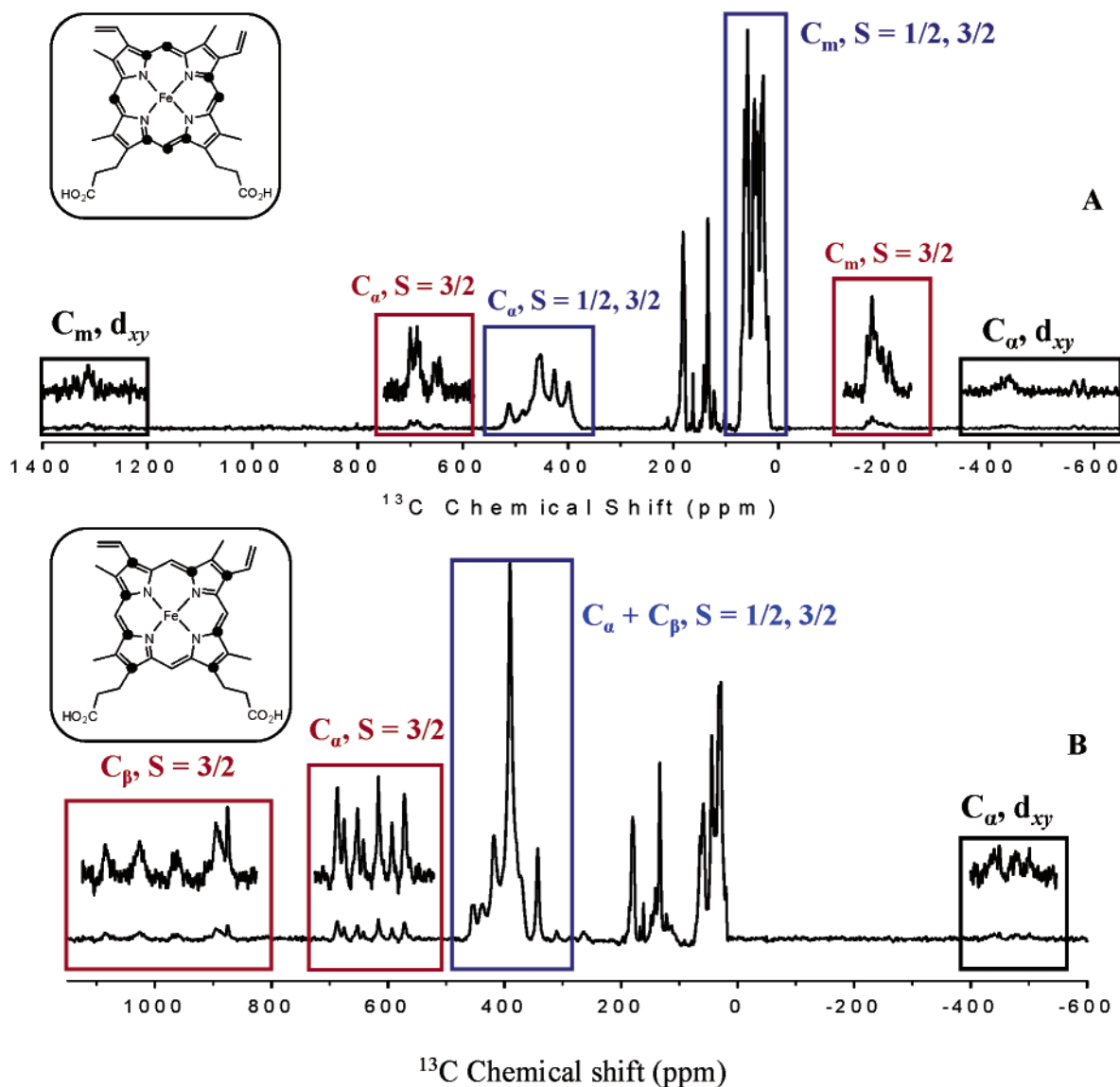


Figure 8. ^{13}C NMR spectra (37 °C) of the $\text{Fe}^{\text{III}}\text{-OH}$ complex of *pa*-HO (pH 10.3) reconstituted with heme labeled at the C_α and C_m (A) and C_α and C_β carbons (B). Peaks corresponding to the population exhibiting the $S = 1/2, 3/2$ spin state crossover are highlighted by blue boxes, and peaks corresponding to the population with the $S = 3/2$ spin state are highlighted by red boxes.

C_α and C_m carbons. In this spectrum, there are two new sets of peaks, one at ca. 1300 ppm and the other at ca. -500 ppm, in addition to the resonances corresponding to the $S = 1/2, S = 3/2$ spin crossover (blue box) and those corresponding to the population exhibiting the pure $S = 3/2$ spin state (red box). The significance of the resonances near 1300 ppm and -500 ppm is made clear once the ^{13}C spectrum of the $\text{Fe}^{\text{III}}\text{-OH}$ complex reconstituted with heme labeled at C_α and C_β carbons is considered. This spectrum (Figure 8B) reveals the presence of a set of peaks at ca. -500 ppm, which can be attributed to C_α carbons on the basis that the spectrum of $\text{Fe}^{\text{III}}\text{-OH}$ labeled at the C_α and C_m carbons (Figure 8A) also displays peaks near -500 ppm. Consequently, the peaks near 1300 ppm in the spectrum of Figure 8A must originate from C_m carbons. Large downfield C_m shifts (500–1300 ppm) and large upfield C_α shifts (-400 to -600 ppm) are diagnostic of $\text{Fe}^{\text{III}}\text{-porphyrinates}$ exhibiting the low-spin (d_{xy})¹ electronic structure.^{12,24} These characteristically large downfield C_m shifts result from unpaired electron density delocalization from the iron d_{xy} orbital into the

porphyrin $3a_{2u}(\pi)$ orbital,¹³ and the large upfield C_α shifts are a consequence of spin polarization from neighboring meso carbons.²⁴ Thus, the peaks at 1300 and -500 ppm in Figure 8A and B, respectively, indicate the presence of a population exhibiting the unusual (d_{xy})¹ electronic structure.

It is important to note that when CN^- is added to the $\text{Fe}^{\text{III}}\text{-OH}$ complex of *pa*-HO at pH 10.3, the ^{13}C NMR spectrum of the resultant $\text{Fe}^{\text{III}}\text{-CN}$ complex does not display the peaks originating from the major population with the $S = 1/2, S = 3/2$ spin state crossover or from the minor populations with the $S = 3/2$ and $S = 1/2$ (d_{xy})¹ spin states (see Figure S2). Instead, the spectrum is almost identical to that exhibited by the $\text{Fe}^{\text{III}}\text{-CN}$ complex at pH 7.0, which has been shown to be $S = 1/2, d_{\pi}$. It is therefore apparent that the ^{13}C resonances in Figures 5, 7, and 8, which have been attributed to the presence of different populations with unusual spin states, are only present when hydroxide is coordinated in the distal site of *pa*-HO. Therefore, it is reasonable to conclude that the $\text{Fe}^{\text{III}}\text{-OH}$ complex of *pa*-HO exists as a mixture of multiple (at least three) conformers,

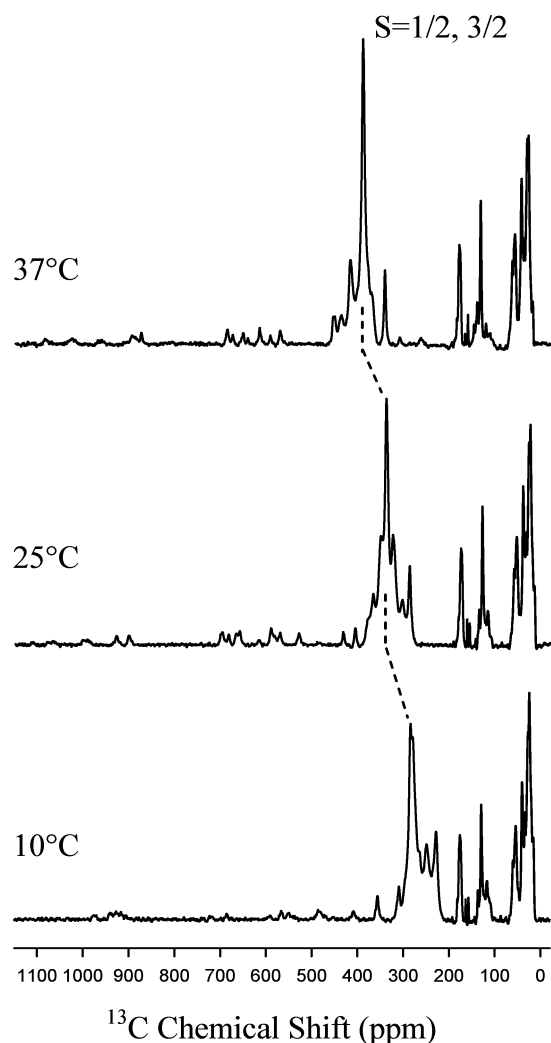


Figure 9. ¹³C NMR spectra of the Fe^{III}–OH complex of *pa*-HO obtained at different temperatures. The temperature dependence of the major population exhibiting the spin crossover between $S = 1/2$ and $S = 3/2$ spin states is highlighted by a dotted line. The downfield peaks correspond to the minor population with the $S = 3/2$ spin state.

each exhibiting a different spin state, and probably different degrees of nonplanar distortions. At 37 °C, the major population exhibiting the $S = 1/2$, $S = 3/2$ spin state crossover accounts for approximately 88% of the total population, whereas those species exhibiting the $S = 3/2$ and the $S = 1/2$ (d_{xy})¹ electronic configurations account for ~10% and ~2% of the total population, respectively.

Figure 9 illustrates the temperature dependence of the spectrum obtained from Fe^{III}–OH reconstituted with heme labeled at the C_α and C_β carbons. It has been pointed out (see above) that the resonances corresponding to the population exhibiting the $S = 1/2$, $S = 3/2$ spin state crossover exhibit a pronounced temperature dependence, with these resonances shifting upfield from ca. 400 ppm at 37 °C to ca. 250 ppm at 0 °C. The magnitude of the temperature-dependent shifts and the fact that the chemical shifts move in the direction of those expected for the planar, low-spin d_{π} complexes suggest that low temperatures decrease the conformational flexibility of the heme pocket and shift the equilibrium toward the planar, $S = 1/2$, d_{π} electronic configuration. At this time, it is not possible to ascertain whether the $S = 1/2$, d_{π} and $S = 3/2$ spin states are

quantum mechanically admixed or simply in fast exchange relative to the NMR time scale. Assuming fast exchange relative to the NMR time scale, we could estimate that the rate of exchange should be faster than $2.7 \times 10^5 \text{ s}^{-1}$. This value was estimated at 37 °C from the difference in shifts between the C_β carbons in the pure $S = 3/2$ spin state (~1000 ppm) and the C_β carbons in the pure $S = 1/2$, d_{π} spin state (~200 ppm). The resonances corresponding to the population with the pure $S = 3/2$ spin state, C_α carbons at ca. 650 ppm and C_β carbons at ca. 1000 ppm, exhibit a significantly less pronounced shift as the temperature is lowered. However, it is interesting to note that these resonances become less intense as the temperature is lowered and are undetectable below 10 °C. This behavior suggests that the populations with the highly nonplanar $S = 1/2$, (d_{xy})¹ and $S = 3/2$ electronic configurations are in slow exchange with the major population exhibiting the $S = 1/2$, $S = 3/2$ crossover. For chemical exchange to be slow relative to the NMR time scale, the exchange has to be much slower than $2.7 \times 10^5 \text{ s}^{-1}$. Thus, as the temperature is lowered, and the conformational flexibility of the heme binding site is decreased, these populations with highly nonplanar porphyrins decrease as the equilibrium shifts toward the planar $S = 1/2$, d_{π} electronic configuration.

Shelnutt has pointed out that multiple conformers can occur for biological porphyrins because several potential energy minima can result from the protein environment.³⁶ The observations described above, therefore, are in agreement with this prediction and imply that in the confines of the protein the relative energy of the porphyrin conformers, as well as the barriers of interconversion, can be modulated by the protein and by the spin state of the macrocycle.

Relevance to the Mechanism of Heme Hydroxylation Carried Out by HO. Axial ligand–metalloporphyrin interactions, among other things, are known to induce nonplanar distortions of the porphyrin ring.^{30,37,38} For instance, it is well documented that the coordination of ligands that are poor σ -donors and good π -acceptors induces significant porphyrin ruffling and stabilization of the (d_{xy})¹ electronic configuration.^{13,15,25,39} Furthermore, crystal field theory indicates that decreasing axial ligand field strength leads to a transition from a low-spin to a high-spin state. The $S = 3/2$ spin state is stabilized when the d_z^2 orbital is singly occupied and relatively close in energy to the d_{xy} , d_{xz} , and d_{yz} orbitals, and the $d_{x^2-y^2}$ orbital is vacant and at significantly higher energy.^{30,40,41} The $d_{x^2-y^2}$ orbital can be destabilized further by increasing the field strength of the equatorial ligand (porphyrin), a strategy that has been utilized by Simonato and co-workers to stabilize the $S = 3/2$ spin state of model ferrihemes.³⁰ Moreover, as the axial ligand field strength is decreased, a compensating increase in equatorial field strength occurs; the increase in equatorial field strength, in turn, typically results in shorter Fe–N_p bond lengths and induces nonplanar distortions of the macrocycle. Therefore, axial ligands

- (36) Shelnutt, J. A. *J. Porphyrins Phthalocyanines* **2000**, *4*, 386–389.
 (37) Shelnutt, J. A.; Song, X. Z.; Ma, J. G.; Jia, S. L.; Jentzen, W.; Medforth, C. J. *Chem. Soc. Rev.* **1998**, *27*, 31–41.
 (38) Roberts, S. A.; Weichsel, A.; Qiu, Y.; Shelnutt, J. A.; Walker, F. A.; Montfort, W. R. *Biochemistry* **2001**, *40*, 11327–11337.
 (39) Guillmot, M.; Simonneaux, G. *J. Chem. Soc., Chem. Commun.* **1995**, 2093–2094.
 (40) Reed, C. A.; Mashiko, T.; Bentley, S. P.; Kastner, M. E.; Scheidt, W. R.; Spartalian, K.; Lang, G. *J. Am. Chem. Soc.* **1979**, *101*, 2948–2958.
 (41) Cheng, R.-J.; Chen, P.-Y.; Gau, P.-R.; Chen, C.-C.; Peng, S.-M. *J. Am. Chem. Soc.* **1997**, *119*, 2563–2569.

with the appropriate field strength are capable of stabilizing the unusual $S = 1/2$, (d_{xy})¹ and $S = 3/2$ spin states, which are typically associated with large nonplanar distortions of the porphyrin ring.

It is evident from the ¹³C NMR spectra discussed above that the hydroxide ligand in the Fe^{III}–OH complex of *pa*-HO encourages the stabilization of the d_z^2 and the destabilization of the $d_{x^2-y^2}$ orbital, hence giving rise to two minor populations exhibiting a pure $S = 1/2$, (d_{xy})¹ and a pure $S = 3/2$ electronic configuration and a major population exhibiting a spin crossover between $S = 1/2$ and $S = 3/2$. It is noteworthy that these observations are in striking contrast to those made with the hydroxide complex of globins, in that the complexation of a hydroxide ligand results in the formation of $S = 1/2$, d_{π} globin complexes.²² A plausible explanation for the unusual behavior of the hydroxide complex of HO stems from at least two unique chemical properties shared by all known HO enzymes: (1) the presence of a well-organized hydrogen-bonding network in the distal site, and (2) the conformational flexibility of the heme binding domain. The relevance of these properties is discussed below.

(1) In addition to heme pocket flexibility (discussed below), the chemical nature of the distal pocket is likely to contribute significantly to the properties exhibited by the Fe^{III}–OH complex. In this context, the distal pocket in heme oxygenase enzymes supports an extensive and well-defined network of hydrogen-bonded water molecules.^{8,10,42} It is possible that one of these water molecules, by virtue of donating a hydrogen bond to the coordinated OH[−] ligand, decreases its σ -donating ability and thereby lowers its field strength. As has been discussed above, lowering the axial ligand field strength leads to the stabilization of the d_z^2 orbital and is also accompanied by a strengthening of the equatorial field. The latter induces nonplanar heme distortions and further destabilization of the $d_{x^2-y^2}$ orbital. It is thus conceivable that the ligand field strength of the coordinated hydroxide, which in HO is modulated by accepting a H-bond from the distal network of water molecules, induces the stabilization of these unusual electronic configurations and nonplanar porphyrin conformations. (2) The different populations with their different electronic configurations and likely different types of nonplanar distortions appear to be in slow exchange with one another relative to the NMR time scale. The relatively slow rate of interconversion between populations with different types of nonplanar distortions is likely a consequence of obligatory accompanying conformational changes in the heme pocket. Thus, the flexibility of the pocket in HO facilitates the relatively large nonplanar heme distortions induced by the binding of hydroxide. At the same time, heme–polypeptide interactions slow the rate of interconversion between the different types of distortions (populations) relative to the interconversion of Fe^{III}–porphyrinates not bound to a protein, such that it becomes possible to observe the different populations

(42) Li, Y.; Syvitski, R. T.; Auclair, K.; Wilks, A.; Ortiz de Montellano, P. R.; La Mar, G. N. *J. Biol. Chem.* **2002**, *277*, 33018–33031.

of HO complexes in slow exchange. By comparison, the more rigid heme binding site of the globins does not facilitate relatively large nonplanar distortions of the heme; therefore, the binding of hydroxide results in the formation of a homogeneous population of nearly planar low-spin d_{π} complexes.

It is apparent that the above-described properties of HO must act in synergism so that the distal network of water molecules serves to lower the ligand field strength of the coordinated peroxide, thus providing the necessary impetus for the heme to deform from planarity. This impetus is reinforced by the flexibility of the distal pocket in HO, which facilitates the conformational changes “dictated” by the field strength of the coordinated hydroxide.

These findings suggest that if the field strength of the hydroperoxide ligand in the Fe^{III}–OOH intermediate could also be modulated by the distal network of hydrogen bonds, significant nonplanar deformations and large spin density at the meso carbons can indeed be expected for this complex. Thus, the efficient meso carbon hydroxylation reaction carried out by HO enzymes is likely a consequence of the chemical non-innocence of the macrocycle. Indeed, if this concept is operative in HO catalysis, it would expand the role currently attributed to the highly organized hydrogen-bond network in the distal pocket of HO to include modulation of the HOO[−] ligand field strength. ENDOR spectroscopic studies have demonstrated that this hydrogen-bond network efficiently delivers a proton to the terminal oxygen of Fe^{III}–OO[−] to form the activated Fe^{III}–OOH intermediate.⁶ The same study reported a second well-defined ¹H signal (denoted H2), which only appears in the ENDOR spectrum upon annealing of the Fe^{III}–OOH intermediate to 200 K, and suggested that proton H2 is part of the activation that leads to meso hydroxylation.⁶ We propose that proton H2, by virtue of forming a hydrogen bond with the coordinated oxygen in Fe^{III}–OOH, can modulate the field strength of the hydroperoxo (hydroxo in the present studies) ligand and consequently induce the unusual spin states and nonplanar distortions that can make the heme macrocycle an active participant in its own hydroxylation.

Acknowledgment. This work was supported by NIH grants GM-50503 (M.R.) and AI-48551 (A.W.), and OCAST grant HR00-043 (M.R.).

Supporting Information Available: Figure S1, variable temperature ¹³C NMR spectra obtained from the Fe^{III}–OH complex of *pa*-HO reconstituted with heme labeled at the C_α and C_m carbons. Figure S2, Top: ¹³C NMR spectrum of the hydroxide complex of *pa*-HO at pH 10.3. Bottom: ¹³C NMR spectrum of the cyanide complex of *pa*-HO obtained at pH 10.3 (PDF). This material is available free of charge via the Internet at <http://pubs.acs.org>.

JA036147I